Alternate Assemblies of Platinum Nanoparticles and Metalloporphyrins as Tunable Electrocatalysts for Dioxygen Reduction

Minghua Huang, Yong Shao, Xuping Sun, Hongjun Chen, Baifeng Liu, and Shaojun Dong*

State Key Laboratory of Electroanalytical Chemistry, Changchun Institute of Applied Chemistry, Chinese Academy of Sciences, Changchun, Jilin 130022, China

Received July 4, 2004. In Final Form: September 29, 2004

Through electrostatic layer-by-layer (LBL) assembly, negatively charged citrate-stabilized platinum nanoparticles (PtNPs) and positively charged [tetrakis(*N*-methylpyridyl)porphyrinato] cobalt were alternately deposited on a 4-aminobenzoic acid-modified glassy carbon electrode and also on indium tin oxide substrates, directly forming the three-dimensional nanostructured materials. Thus-prepared multilayer films were characterized by UV−visible spectroscopy, surface plasmon resonance (SPR) spectroscopy, atomic force microscopy (AFM), and cyclic voltammetry. Regular growth of the multilayer films is monitored by UV−visible spectroscopy and SPR spectroscopy. AFM provides the morphology of the multilayer films. The PtNPs containing multilayer films exhibit high electrocatalytic activity for the reduction of dioxygen with high stability. Rotating disk electrode voltammetry and rotating ring−disk electrode voltammetry demonstrate that the PtNP-containing multilayer films can catalyze an almost four-electron reduction of O_2 to H_2O in an air-saturated 0.5 M H_2SO_4 solution. Furthermore, the electrocatalytic activity of the films could be further tailored by simply choosing different cycles in the LBL process or more specifically the amount of the assembly components in the films. The high electrocatalytic activity and good stability for dioxygen reduction make the PtNP-containing multilayer films potential candidates for the efficient cathode material in fuel cells.

1. Introduction

Interest in fuel cell technology has motivated the search for a cheap and an effective cathode material that can accomplish the direct four-electron reduction of dioxygen to water.[1,2] As a result of nanoparticles exhibiting a range of physical and chemical properties that are promising for potential applications in a new generation of optical, electronic, and chemical devices, the search for highly effective catalysts has spanned to the exploration of nanometer-sized catalysts. Metal nanoparticle-modified electrodes are used increasingly in many electrochemical applications owing to their extraordinary catalytic properties over bulk-metal electrodes.[3,4] For the reduction of dioxygen, of numerous catalysts, Pt and Pt-based materials are still indispensable and the most effective catalyst that supports predominantly the direct four-electron reduction dioxygen to water.[5,6] The rational and efficient use of Pt is important because of its high cost and limited supply. As a result, Pt nanoparticles (PtNPs) have been an intensive research subject for the design of inexpensive cathode material.[7] There are several methods for preparing Pt metal clusters on solid supports including electroless deposition,[5,7,8] the electrochemical process,[9] the radio frequency method,[10] and metal evaporation.[11] Most of the above methods are preformed on the deposition of Pt at the solid supports from platinum salt solutions or metal Pt. Compared with these strategies to nanoparticle arrays, the wet chemical approach provides an easier control over island size and shape by nanoparticle synthesis chemistry.[12] Very few papers have reported the self-assembly of multilayer films containing PtNPs with its narrow size distribution from pre-synthesized nanoparticles through reduction of metal salts by reducing agents in solution.[13,14]

In recent years, a well-established electrostatic layer-by-layer (LBL) self-assembly technique initially developed for pairs of oppositely charged polyelectrolytes[15] provides a viable approach for the formation of three-dimensional (3D) nanostructured thin films with many fascinating properties in a controlled, defined manner.[16,17] The methods allow for the fabrication of robust, homogeneous films with a fine controlled film thickness and amount of the components. The general utility and vitality of these systems are further broadened when quantum dots and nanoparticles are incorporated into these multilayer films.

* To whom correspondence should be addressed. Fax: (+86)-431-5689711. E-mail: dongsj@ns.ciac.jl.cn.

(1) Prakash, J.; Joachin, H. *Electrochim. Acta* **2000**, *45*, 2289.
(2) Paulus, U. A.; Schmidt, T. J.; Gasteiger, H. A.; Behm, R. J. *J. Electroanal. Chem*. **2001**, *495*, 134.
(3) El-Deab, M. S.; Ohsaka, T. *Electrochem. Commun*. **2002**, *4*, 288.
(4) Luo, J.; Lou. Y.; Maye, M. M.; Zhong, C. J.; Hepel, M. *Electrochem. Commun*. **2001**, *3*, 172.
(5) Brussel, M. V.; Kokkinidis, G.; Vandendael, I.; Buess-Herman, C. *Electrochem. Commun*. **2002**, *4*, 808
(6) Coutanceau, C.; Croissant, M. J.; Napporn, T.; Lamy, C. *Electrochim. Acta* **2000**, *46*, 579.
(7) Brussel, M. V.; Kokkinidis, G.; Hubin, A.; Buess-Herman, C. *Electrochim. Acta*. **2003**, *48*, 3909.
(8) Kokkinidis, G.; Papoutsis, A.; Stoychev, D.; Milchev, A. *J. Electroanal. Chem*. **2000**, *486*, 48.
(9) Zoval, J. V.; Lee, J.; Gorer, S.; Penner, R. M. *J. Phys. Chem. B* **1998**, *102*, 1166.
(10) Yan, T.; Niwa, O.; Horiuchi, T.; Tomita, M.; Iwasaki, Y.; Ueno, Y.; Hirono, S. *Chem. Mater*. **2002**, *14*, 4796.
(11) Klabunde, K. J.; Li, Y. X.; Tan, B. J. *Chem. Mater*. **1991**, *3*, 30.
(12) Grabar, K. C.; Freeman, R. G.; Hommer, M. B.; Natan, M. J. *Anal. Chem*. **1995**, *67*, 735.
(13) Ghannoum, S.; Xin, Y.; Jaber, J.; Halaoui, L. I. *Langmuir* **2003**, *19*, 4804.
(14) Horswell, S. L.; O'Neil, I. A.; Schiffrin, D. J. *J. Phys. Chem. B* **2003**, *107*, 4844.
(15) Decher, G. *Science* **1997**, *277*, 1232.
(16) Liu, S.; Kurth, D. G.; Möhwald, H.; Volkmer, D. *Adv. Mater*. **2002**, *14*, 225.
(17) Cheng. L.; Cox, J. A. *Chem. Mater*. **2002**, *14*, 6.

10.1021/la048337s CCC: $30.25
Published on Web 12/07/2004

Usually, 3D multilayer films of charged nanoparticles were assembled by virtue of oppositely charged polyelectrolytes in a cyclic deposition fashion.[18] 3D nanoparticle multilayer films can also be assembled by virtue of a molecular cross-linker in an analogous way to the LBL assemblies of nanoparticles/polyelectrolytes.[19] The driving force for molecularly linked nanoparticle multilayer films can be electrostatic interaction, covalent bonding, or both.

Metalloporphyrin molecules have been widely used as effective catalysts for dioxygen reduction. This is also the main reason that metalloporphyrins were selected as molecule cross-linkers to construct the desired nanostructured materials. Considerable efforts have been devoted to the design and controlled fabrication of metalloporphyrin-modified films.[20,21] Unfortunately, the catalytic activity of these metalloporphyrins is neither durable nor stable for dioxygen reduction. Incorporating such functional units into high-surface-area surface-confined nanostructured thin films with high stability using LBL assembly might be significant for sensoric applications.

Here, we prepared 3D PtNPs/[tetrakis(*N*-methylpyridyl)porphyrinato] cobalt (CoTMPyP) nanostructured materials by the electrostatic LBL self-assembly. The electrostatic interaction between negatively charged citrate-stabilized PtNPs and positively charged CoTMPyP is strong enough to drive the formation of the 3D nanostructured materials. Rotating disk electrode (RDE) voltammetry and rotating ring−disk electrode (RRDE) voltammetry demonstrate that the PtNP-containing multilayer films can catalyze an almost four-electron reduction of O_2 to H_2O in air-saturated 0.5 M H_2SO_4. Interestingly, we note that the electrocatalytic activity of the multilayer films for dioxygen reduction was highly tunable by choosing different cycles in the LBL process or more specifically the amount of assembly components in the films. The PtNP-containing multilayer films exhibit slightly higher current density and more positive potential for dioxyen reduction, compared with the bulk Pt electrode. The high electrocatalytic activity and good stability for dioxygen reduction make the PtNP-containing multilayer films potential candidates for the efficient cathode material in fuel cells.

2. Experimental Section

2.1. Materials. 4-Aminobenzoic acid (4-ABA) was purchased from Aldrich. The absolute ethanol was dried over 3-Å molecular sieves before use, and lithium perchlorate was dried at about 90 °C in a vacuum oven before use. CoTMPyP$(ClO_4)_5$ was synthesized as previously reported.[22] $H_2PtCl_6{\cdot}6H_2O$, H_2SO_4, and other chemicals were of analytical reagent grade and used as received. Water used for the preparation of aqueous solution was purified using a Milli-Q water purification system. Buffer solutions were 0.1 M NaAc + HAc (pH = 3.64).

2.2. Synthesis of Citrate-Stabilized PtNPs. A total of 1 mL of 1% H_2PtCl_6 aqueous solution was added into 100 mL of water and then heated to boiling. Aging of the H_2PtCl_6 solution was not necessary in this synthetic procedure. Then 3 mL of a 1% sodium citrate aqueous solution was added rapidly, and the mixture was kept at boiling temperature for about 30 min. Transmission electron microscopy was used to examine the particle size distribution, and an average diameter of 6 nm was confirmed (the figure is not shown).

2.3. Preparation Procedure of the Multilayer Films Containing PtNPs. A glassy carbon electrode (GCE) was first treated with 4-ABA according to the published procedures.[23,24] Then, the 4-ABA/GCE was immersed in 0.5 mM CoTMPyP + 0.1 M acetate buffer (pH = 3.64) with cyclic potential scanning between 0.2 and −0.4 V at a scan rate of 100 mV s^{-1} for 100 cycles. After thoroughly rinsing with water and drying with nitrogen stream, the modified electrode with a CoTMPyP layer was transferred to citrate-stabilized PtNP solution for 20 min resulting in one layer of PtNPs. When the resulting modified electrode was alternately placed in CoTMPyP and PtNP solutions in an electrostatic fashion, the multilayer films could be formed. The thickness of the multilayer films was readily adjusted by choosing a different number of cycles by the LBL modification method.

2.4. Characterization of the Multilayer Films Containing PtNPs. Electrochemical experiments were performed with a CHI 660 electrochemical workstation (U.S.A.) in a conventional three-electrode electrochemical cell using GCE (3-mm diameter) as the working electrode, twisted platinum wire as the auxiliary electrode, and an Ag/AgCl reference electrode in aqueous media or Ag/Ag^+ (0.01 M $AgNO_3$) in anhydrous ethanol solutions. The GCEs were polished with 1.0 and 0.3 μm α-Al_2O_3 powders, successively, and sonicated in water for about 3 min after each polishing step. Finally, the electrodes were sonicated in ethanol, washed with ethanol, and dried with a high-purity nitrogen stream immediately before use. Solutions were deaerated for at least 20 min with a high-purity nitrogen stream and kept under a pressure of this gas during the experiments.

An EG & PARC model 636 rotating ring−disk electrode system and an EG & PARC model 366 bipotentiostat were used for RDE and RRDE voltammetry experiments. A rotating GC disk-platinum ring electrode was used as a working electrode. The collection efficiency (N) of the ring electrode obtained by reducing ferricyanide at a disk electrode was 0.193.

UV−vis absorption spectra were recorded using a Cary 500 Scan UV−vis−NIR spectrometer (Varian Co.) on a transparent indium tin oxide (ITO) glass substrate, which was sonicated in acetone for 5 min, followed by rinsing with water, ultrasonic agitation in concentrated NaOH in 1:1 (v/v) water/ethanol, rinsing further with water, immersion in $CHCl_3$ for 10 min, and drying with a high-purity nitrogen stream according to the a known process.[25] UV−vis measurement was performed on an ITO-coated glass substrate assembled with PtNPs and CoTMPyP multilayer films in a manner similar to the above procedure. The resulting films were washed with water, dried under nitrogen, and used to record UV−vis spectra to follow the deposition processes. The spectra were background-subtracted from a reference sample of a bare ITO substrate.

The substrate for surface plasmon resonance (SPR) experiments was prepared by the solution-based electroless plating of a about 50-nm gold films onto macroscope slides according to the published procedures.[26] The as-prepared gold film substrate was pressed onto the base of a half cylindrical lens (n = 1.61) via an index-matching oil. Linearly p-polarized light having a wavelength of 670 nm from a diode laser was directed through the prism onto the gold film in the Kretshmann configuration by using a SPR apparatus (SPR 2000, the Institute of electronics, Chinese Academy of Sciences, China). The intensity of the reflected light was measured as a function of the angle of incidence, θ, using a photodiode with a chopper/lock-in amplifier technique. For SPR, the as-prepared gold film substrates were mounted against the Teflon cuvette with a 1-mL volume using a Kalrez O-ring, which provides a liquid-tight seal for the electrolyte contact. Before LBL assembly, the Au/glass substrate was first exposed to a freshly prepared aqueous solution of

(18) Caruso, F.; Caruso, R. A.; Mohwald, H. *Science* **1998**, *282*, 1111. (b) Gao, M. Y.; Richter, B.; Kirstein, S.; Mohwald, H. *J. Phys. Chem. B* **1998**, *102*, 4096.

(19) Shipway, A. N.; Katz, E.; Willner, I. *ChemPhysChem* **2000**, 1, 18.

(20) Boeckl, M. S.; Bramblett, A. L.; Hauch, K. D.; Sasaki, T.; Ratner, B. D.; Rogers, J. W. *Langmuir* **2000**, *16*, 5644.

(21) Sharma, C. V. K.; Broker, G. A.; Szulczewski, G. J.; Rogers, R. D. *Chem. Commun*. **2000**, 1023.

(22) Pasternack, R. F.; Cobb, M. S. *J. Inorg. Nucl. Chem*. **1973**, *35*, 4327.

(23) Liu, J. Y.; Cheng, L.; Liu, B. F.; Dong, S. J. *Langmuir* **2000**, *16*, 7471.

(24) Cheng, L.; Liu, J. Y.; Dong, S. J. *Anal. Chim. Acta* **2000**, *417*, 133.

(25) Prieto, I.; Martin, M. T.; Möbius, D.; Camacho, L. *J. Phys. Chem. B* **1998**, *102*, 2523.

(26) Jin, Y. D.; Kang, X. F.; Song, Y. H.; Cheng, G. J.; Dong, S. J. *Anal. Chem*. **2001**, *73*, 2843.

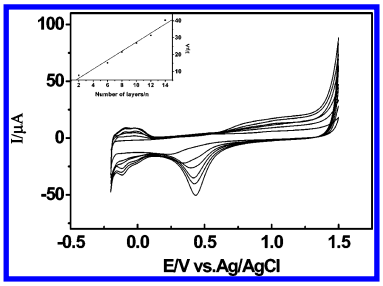

Figure 1. CVs of the multilayer films containing PtNPs (PtNPs as the outmost layer) with different numbers of layers: $n = 2$, 6, 8, 10, 12, and 14 (from inside to outside), respectively. Supporting electrolyte, 0.5 M H_2SO_4 solution; scan rate, 50 mV s^{-1}.

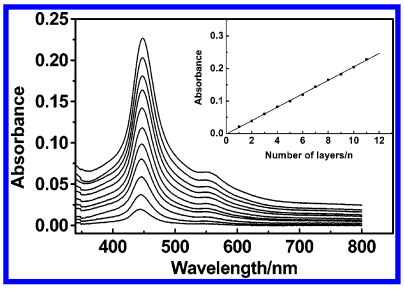

Figure 2. UV−vis absorption spectra of the PtNP and CoTMPyP multilayer films on the ITO substrate (CoTMPyP as the outmost layer) with different numbers of layers: 1, 2, 3, ..., and 11 (curves from bottom to top, respectively). The inset shows the relationship of absorbance at 445 nm versus the layer numbers.

3-mercaptopropionic acid to form a carboxyl-terminated monolayer. SPR measurement was performed on the as-pretreated gold film substrate assembled with PtNPs and CoTMPyP multilayer films in a manner similar to the above procedure.

Atomic force microscopy (AFM) measurements were performed on the GCE with a SPI3800N microscope (Seiko Instruments, Inc.). The images were acquired in the tapping mode. Measurements were made with the Si cantilever in air at room temperature. The force constant of the cantilever was 0.1−0.6 N/m with scan rate of 1−2 Hz.

3. Results and Discussion

3.1. Fabrication of the PtNP and CoTMPyP Multilayer Films on 4-ABA-Modified GCE. The electrostatic attraction between negatively charged citrate-stabilized PtNPs and positively charged CoTMPyP was used as the driving force to build up the 3D multilayer films. Through the attachment of the 4-ABA-containing COOH group to the GCE, the 4-ABA-modified GCE was alternately immersed in CoTMPyP solutions with cyclic potential scanning in a suitable potential range and PtNPs. With PtNPs as the redox-active species, the multilayer deposition process on the above-mentioned modified GCE was monitored by cyclic voltammetry. Figure 1 shows representative cyclic voltammograms (CVs) obtained from −0.2 to +1.5 V at the multilayer films containing a PtNP electrode (PtNPs as the outmost layer) with different numbers of PtNP layers in 0.5 M H_2SO_4 solution. It can be seen that the voltammograms are similar to that of a polycrystalline Pt electrode,[27] displaying the characteristic anodic−cathodic current profile in which near-reversible peaks below 0 V associated with hydrogen desorption−adsorption and the irreversible features corresponding to the formation and removal of platinum surface oxide are observed. Furthermore, it can be seen that with the increase of PtNP layers the onset of the oxide formation and the peak potential of the oxide reduction are shifted to more positive, indicating that the increase of PtNP amounts inhibits the chemisorptions of OH on the Pt sites,[28] which may have a beneficial effect on the oxygen adsorption at a low overpotential and, thus, may lead to improvement in dioxygen reduction kinetics.[28,29] In addition, with the number of PtNP layers deposited increasing, the redox peak currents increase gradually. Taking the platinum oxide reduction peak at about 0.4 V as an example, a good linear relationship between the layer numbers and the cathodic peak currents of PtNPs, as shown in the inset of Figure 1, demonstrates that equal amounts of PtNPs are adsorbed in each deposition cycle, also confirming that the film grows uniformly.

3.2. UV−Visible (UV−Vis) Absorption Spectroscopy Characterization. As a result of the absorption intensity being proportional to the concentration of the deposition material with characteristic absorption peaks in the UV−vis region, the growth process of the multilayer films can be monitored by UV−vis spectroscopy. Figure 2 shows the UV−vis absorption spectra of the PtNP and CoTMPyP multilayer films with different layer numbers, and CoTMPyP existed in the outmost layer. It can be seen that the absorption of the PtNPs and CoTMPyP multilayer films occurs at the same wavelenghs with sequential deposition. The absorbance at 445 nm corresponding to the porphyrin soret band is observed to increase linearly with the number of layers as shown in the inset of Figure 2. The linear increase of the intensity of the absorption peaks as a function of the number of layers indicates that a regular and uniform multilayer film has been constructed, which is consistent with a well-behaved LBL assembly process as described previously.[30] The soret absorption peaks of metalloporphyrins in the multilayer films show red shift by about 10 nm as compared to that in solution, which results from the formation of aggregates of chromophores within the layers.[31]

3.3. SPR Measurement. The SPR technique is extremely sensitive to the refractive index change of layers presented in the sensor surface.[32] Here, we applied the SPR spectroscopy to monitor the growth of the multilayer films. Figure 3A shows the scanning SPR spectra of the 3-mercaptopropionic acid-modified gold electrode (curve a), sequential 20-min adsorption of CoTMPyP cations (curve b), and another 20-min adsorption of PtNPs (curve c). All the spectra were recorded in pure water after thoroughly rinsing to remove weakly bound species. After formation of the first CoTMPyP layer, the reflectance minimum is right-shifted by about 0.32° in comparison to the basal surface. Upon adsorption of the PtNPs layer to the positively charged CoTMPyP layer, another right-shift in the reflectance minimum by about 0.27° occurred. With the increase of the deposition cycles, the SPR reflectance curves shifted toward higher angles, which means that the total thickness of the multilayer films increases by alternately depositing CoTMPyP and PtNPs on the substrate. The changes of the reflectance minimum $\Delta\theta$ are observed to increase linearly with the number of layers

(27) For example: Conway, B. E. *Prog. Surf. Sci.* **1995**, *49*, 331.
(28) Yang, H.; Alonso-Vante, N.; Leger, J.-M.; Lamy, C. *J. Phys. Chem. B* **2004**, *108*, 1938.
(29) Paulus, U. A.; Wokaun, A.; Scherer, G. G.; Schmidt, T. J.; Stamcnkovic, V.; Markovic, N. M.; Ross, P. N. *Electrochim. Acta* **2002**, *47*, 3787.
(30) Araki, K.; Wagner, M. J.; Wrighton, M. S. *Langmuir* **1996**, *12*, 5393.
(31) Shen, Y.; Liu, J. Y.; Jiang, J. G.; Liu, B. F.; Dong, S. J. *Electroanalysis* **2002**, *14*, 1557.
(32) Raether, H. *Surface Plasmon on Smooth and Rough Surfaces and on Gratingers, Springer Tracts in Modern Physics*; Springer-Verlag: Berlin, 1988; Vol. 11.

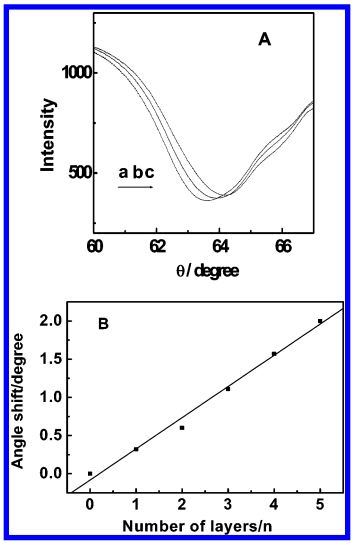

Figure 3. (A) In situ scanning SPR curves of CoTMPyP (curve b) and PtNP (curve c) sequential adsorption on a 3-mercaptopropionic acid (curve a)-modified gold thin-film electrode. All curves were recorded in pure water after washing. (B) Correlation changes of the SPR reflectance minimum, $\Delta\theta$, with the increase of the number of the layers deposited by the LBL method (CoTMPyP as the outmost layer).

as shown in Figure 3B. This indicates that a regular and uniform multilayer film has been constructed, which is consistent with the above results obtained from UV−vis absorption spectroscopy characterization and cyclic voltammetry characterization.

3.4. AFM Measurement. Morphological characterization was conducted by AFM on a bare GCE (Figure 4A), $(PtNPs/CoTMPyP)_1$/4-ABA/GCE (Figure 4B), and $(PtNPs/CoTMPyP)_5$/4-ABA/GCE (Figure 4C). Because of the relatively rough surface of the glassy carbon (GC), the bare GCE exhibits a poor surface morphology with a root-mean-squared roughness of 3.95 nm (Figure 4A). After the immobilization of CoTMPyP and PtNPs, the GCE becomes smoother (Figure 4B,C). It is possible that the CoTMPyP and PtNPs might fill some vacancy and defect of the films. We can also see that while the film thickness increases from one layer to five layers the surface roughness increased from 2.24 to 3.34 nm. In addition, the surface morphology of the $(PtNPs/CoTMPyP)_5$ film comprised individual, uniformly distributed nanoparticles with an average diameter of 10−25 nm, which indicates the multilayer films should be a uniform blend distribution of PtNPs and CoTMPyP. Also, it can be seen that, with increasing the number of layers, the number of density of nanoparticles is enhanced (see parts B and C of Figure 4, respectively).

3.5. Tunable Electrocatalytic Activity of Dioxygen Reduction on the Multilayer Films Containing PtNPs. Of central interest here are the electrocatalytic applications of the multilayer films. We have investigated the electrocatalytic activity of the PtNP-containing multilayer films for dioxygen reduction in detail. Figure 5A presents CVs of the as-prepared multilayer film electrode (PtNPs as the outmost layer) with different layer numbers of PtNPs in the 0.5 M H_2SO_4 solution with and without dioxygen. The dashed line corresponds to the CV of the multilayer film electrode containing two layers of PtNPs (PtNPs as the outmost layer) in N_2-saturated 0.5 M H_2SO_4 solution. In the presence of dioxygen, a remarkable catalytic reduction current at the multilayer film electrode containing 14 layers of PtNPs occurs at 0.49 V, which shifts 390 mV more positive than that of the PtNP

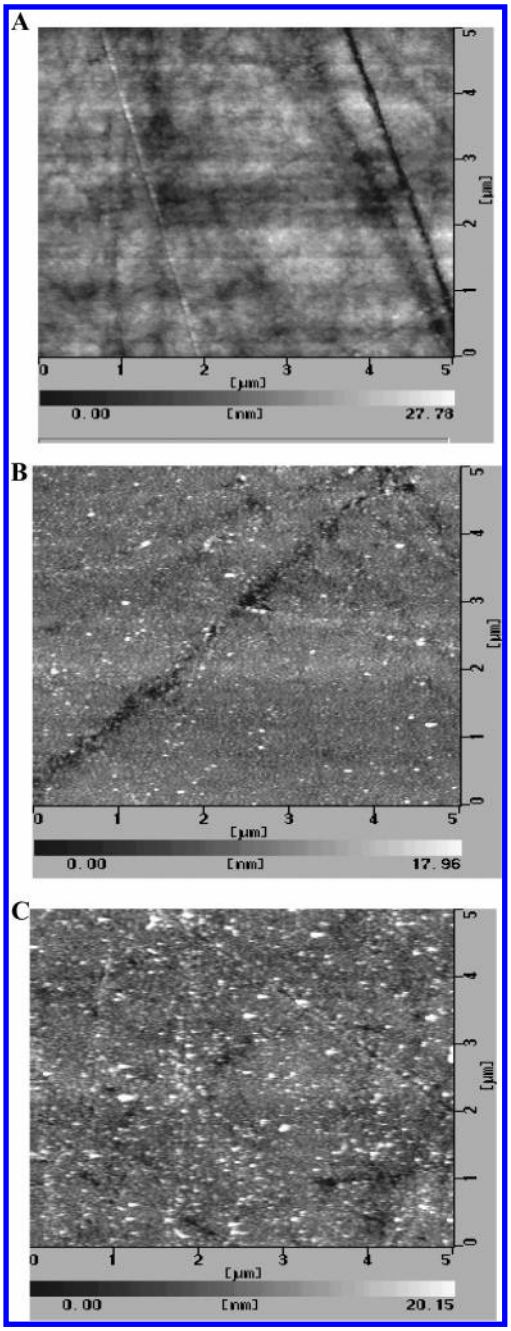

Figure 4. AFM images of a bare GCE (A), $(PtNPs/CoTMPyP)_1$/4-ABA/GCE (B), and $(PtNPs/CoTMPyP)_5$/4-ABA/GCE (C).

monolayer film (0.10 V) as shown in Figure 5A. It also can be seen that, with increasing the number of layers, the catalytic current of dioxygen reduction increases gradually and, interestingly, the reduction peak potential shifts positively. Therefore, by simply choosing different cycles in the LBL assembly process, the film thickness and the amount of assembly components were readily adjusted, while tuning the catalytic activity toward dioxygen reduction. Clearly, the sensitivity of the multilayer films containing 14 layers of PtNPs is higher than that of the PtNP monolayer films. Compared to the multilayer films assembled with CoTMPyP and polyoxometalates,[31] in which only the catalytic current is increased with the increase of the layer numbers while the catalytic peak potential is intact, here the multilayer films containing PtNPs show a positive shift of the catalytic peak potential besides the increase of the catalytic current. It is possible that the PtNPs play an additional role in the dioxygen

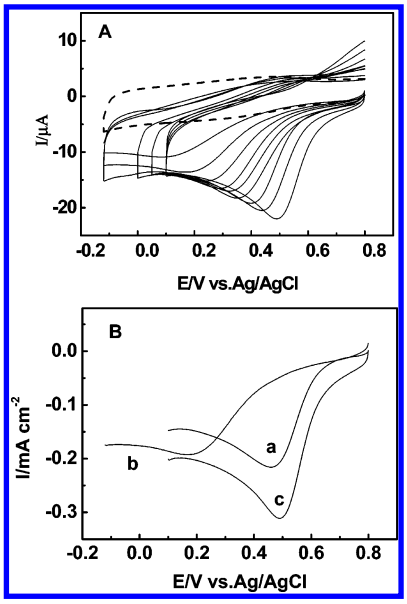

Figure 5. (A) CVs of dioxygen reduction at the multilayer films containing PtNPs (PtNPs as the outermost layer) with different numbers of layers: $n = 1$, 2, 4, 5, 6, 8, 10, 12, and 14 (from top to bottom), respectively. The dashed line corresponds to the CV of the multilayer films containing two layers of PtNPs (PtNPs as the outmost layer) in N_2-saturated 0.5 M H_2SO_4. Supporting electrolyte, air-saturated 0.5 M H_2SO_4 solution; scan rate, 50 mV s^{-1}. (B) Polarization curves for dioxygen reduction at the bulk Pt electrode (curve a) and the multilayer films containing the 2- (curve b) and 14-layer PtNP-modified electrode (curve c) in air-saturated 0.5 M H_2SO_4 solution. Scan rate, 50 mV s^{-1}.

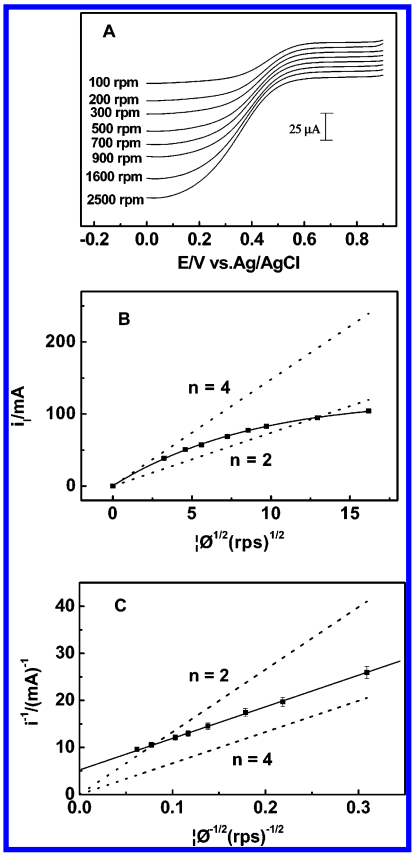

Figure 6. (A) Current−potential curves of dioxygen reduction at a RDE assembled with $(PtNPs/CoTMPyP)_9$ multilayer films with different rotating rates in air-saturated 0.5 M H_2SO_4 solution. Levich plot (B) and Koutecky−Levich plot (C) of the kinetic limiting currents of the voltammogramms. The solid line is from the experimental data, and the dashed lines are from the calculated data considering the reduction of O_2 by two and four electrons, respectively.

reduction process, which might make the electron transfer through the films easier. In addition, because the solubility of dioxygen in the electrolyte is very low, higher PtNP amounts in the films maybe lead to the earlier depletion, thus, also causing the peak potential to appear earlier. In fact, the Caruso group has recently reported that the sensitivity of the gold nanoparticle-containing nanostructured films for measuring NO can be controlled through the film thickness, or more specifically the gold nanoparticle content in the films.[33]

On the other hand, we also compared the electrocatalytic activity for dioxygen reduction at the three kinds of multilayer film electrodes containing the same five layers prepared by the same LBL method, poly(sodium 4-styrenesulfonate) (PSS)/CoTMPyP, PtNPs/poly(diallyldimethylammonium chloride) (PDDA), and PtNPs/CoTMPyP (the figure is not shown). The result showed that the $(PtNPs/CoTMPyP)_5$ multilayer film electrode exhibits higher current than those of the $(PtNPs/PDDA)_5$ and $(PSS)_4/(CoTMPyP)_5$ multilayer film electrodes. Also, it exhibits more positive potential than that of the $(PSS)_4/(CoTMPyP)_5$ multilayer film electrode.

In addition, for the purpose of comparison we have recorded the polarization curves for O_2 reduction on the bulk Pt electrode and the multilayer films containing 2 and 14 layers of PtNPs as shown in Figure 5B. The current densities were the values based on the geometric surface area of the electrode. Before the experiments, the bulk Pt electrode was mechanically polished and scanned in 0.5 M H_2SO_4 at the range of −0.2 to +1.5 V until CV characteristics for a clean Pt electrode were obtained. It can be seen that the current density of the bulk Pt electrode (curve a) is higher than that of the two layers of PtNPs-modified electrode (curve b), and the polarization potential of the former is more positive than that of the latter. However, by increasing the number of cycles to 14 in the LBL process, the catalytic activity is enhanced obviously (curve c), in terms of both the current density and the reduction peak potential. The multilayer films containing the 14 PtNP-modified electrode exhibits a slightly higher current density and more positive polarization potential than those of the bulk Pt electrode, which is possible to save the precious metal Pt.

3.6. Kinetic Analysis of Dioxygen Reduction on the Multilayer Films Containing PtNPs. To quantify the stoichiometry of the catalytic reduction of dioxygen, voltammetric measurements at a RDE and a RRDE have been performed. Figure 6A reveals current−potential curves of dioxygen reduction in air-saturated 0.5 M H_2SO_4 at various rotation rates using the rotating GC disk electrode assembled with the $(PtNPs/CoTMPyP)_9$ multilayer films. It can be seen that potential-independent plateau currents are present at all rotation rates. The Levich and Koutecky−Levich plots obtained from the plateau currents at 0.20 V of Figure 6A are shown in Figure 6B,C, respectively. If solely the mass-transport process in the solution controls the reduction of dioxygen at the PtNP-containing-multilayer-film-modified electrode, the relationship between the limiting current and rotation rate should obey the Levich equation:[34]

$$i_l = i_{Lev} = 0.62nFAc_0D^{2/3}\nu^{-1/6}\omega^{1/2} \quad (1)$$

(33) Yu, A. M.; Liang, Z. J.; Cho, J. H.; Caruso, F. *Nano Lett.* **2003**, *3*, 1203.

where n, A, c_0, D, ν, and ω represent the number of electrons transferred, the electrode area, the bulk concentration of dioxygen in the solution, the dioxygen diffusion coefficient, the kinematic viscosity, and the rotation rate, respectively. From eq 1, the plot of the limiting current i_l as a function of the square root of rotation rate $\omega^{1/2}$ should be a straight line intersecting the origin. From Figure 6B, it is observed that with the increase of the electrode rotation rate, the catalytic current increases gradually and then begins to level off at higher rotation rates. The clear lack of linearity in the Levich plot suggests that the catalytic reaction is limited by kinetics and not by mass transport. The slope of the Levich plot is close to that of the calculated line for the four-electron reduction of O_2. The catalytic current i_{cat} corresponding to the mediated reaction is a function of the Levich current i_{Lev} representing the mass transport of O_2 in the solution and the kinetic current i_K representing the current in the absence of mass transport effect. Andrieux et al.[35] have described the kinetics process of the catalytic reaction at the modified electrodes using the following equation:

$$1/i_l = 1/i_{Lev} + 1/nFAc_0k\Gamma[1 - (i_l d/FAc_p{}^0D_e)] \quad (2)$$

where k, Γ, d, $c_p{}^0$, and D_e are the reaction rate constant, the surface concentration of the catalyst in the film, the film thickness, the total volume concentration of the catalyst in the film, and the diffusion coefficient of electrons in the film, respectively. The other symbols have their usual meanings. When the mass-transport process in the solution and the catalytic reaction become dominant, the term $[1 - (i_l d/FAc_p{}^0D_e)]$ is essentially equal to unity and eq 2 reduces to the Koutecky−Levich equation:[34]

$$1/i_l = 1/nFAc_0k\Gamma + 1/0.62nFAc_0D^{2/3}\nu^{-1/6}\omega^{1/2} \quad (3)$$

$$i_K = nFAc_0k\Gamma \quad (4)$$

As seen from Figure 6C, the Koutecky−Levich plot, from which the number of electrons transferred for the O_2 reduction can be determined, is linear with a slope very close to that of the dashed line calculated for the four-electron reduction of O_2 by a kinetics-controlled process. The calculated number of electrons involved in the reduction of O_2 from the slope of the Koutecky−Levich plot is found to be about 4.0 for the $(PtNPs/CoTMPyP)_9$ multilayer films with the diffusion coefficient of O_2 $D = 1.7 \times 10^{-5}$ cm^2 s^{-1}, the concentration of O_2 in air-saturated 0.5 M H_2SO_4 solution $c_0 = 2.9 \times 10^{-4}$ M, the kinematic viscosity $\nu = 0.01$ cm^2 s^{-1}, and rotating disk area $A = 0.1524$ cm^2. The i_K value obtained from the intercepts of the Koutecky−Levich plot is found to be 0.19 mA. The rate constant, k, calculated from the i_K value, is found to be 1.01×10^4 M^{-1} s^{-1}, which is comparable with those reported previously for the electrocatalytic reduction of dioxygen at the other modified electrodes.[36]

Mass-transport-corrected Tafel plots of E versus $\log[i/(i_l - i)]$ for the PtNP-containing multilayer film electrode at a rotation rate of 2500 rpm in the mixed kinetic-diffusion-controlled region were obtained from the Koutechy−Levich plots as shown in Figure 7. It is well-known that pure Pt shows two Tafel slope regions, in which the small Tafel slope (ca. −60 mV/decade) corresponds to

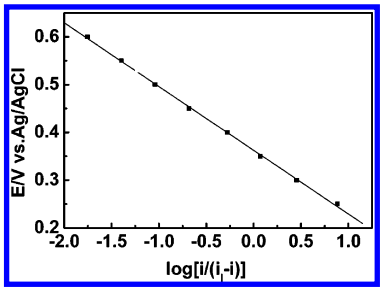

Figure 7. Tafel plots for the dioxygen reduction reaction in air-saturated 0.5 M H_2SO_4 at the $(PtNPs/CoTMPyP)_9$-multilayer-film-modified electrode. The rotation rate is 2500 rpm.

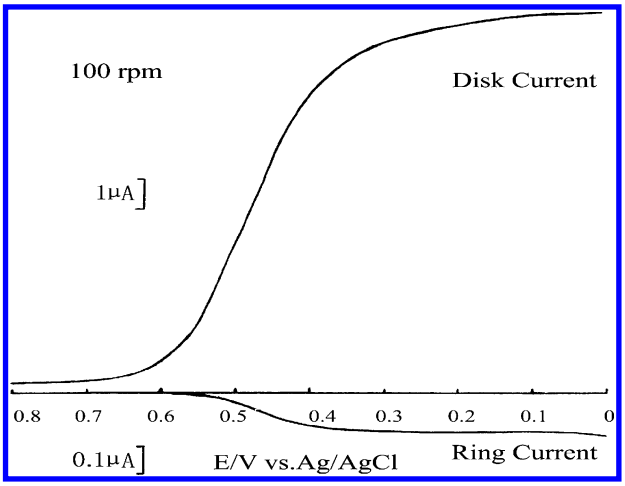

Figure 8. RRDE voltammograms of the $(PtNPs/CoTMPyP)_9$-multilayer-film-modified GCE (disk scan rate, 20 mV s^{-1}; ω, 100 rpm) in the air-saturated 0.5 M H_2SO_4 solution. The potential of the platinum ring electrode was set to 1.0 V to oxidize H_2O_2 to O_2 completely.

O_2 electroreduction at the oxidized (Pt−OH) surface, whereas the large Tafel slope (ca. −120 mV/decade) corresponds to that on a clean Pt surface.[37,38] For the PtNP-containing multilayer films, the Tafel slope was −133 mV/decade. The value is close to the value of −120 mV/decade, similar to that of clean Pt, indicating the first electron-transfer step as the rate-limiting one in the four-electron reduction of dioxygen:

$$O_2 + H^+ + e^- \rightarrow (O-OH)_{adsorbed} \quad (5)$$

A rotating GC disk−platinum ring electrode was employed to determine the quantity of H_2O_2 that was generated by a two-electron reduction process of O_2 at the disk electrode, which provides further supports for the effectiveness of this catalyst for the proposed four-electron reduction of dioxygen. Figure 8 shows the voltammetric curves for dioxygen reduction, recorded at the RRDE with the $(PtNPs/CoTMPyP)_9$ multilayer films immobilized on the GC disk electrode. The disk potential was scanned from 0.8 to 0 V while the ring potential was held at 1.0 V to oxidize the H_2O_2 generated by O_2 reduction at the disk electrode. From Figure 8, the large disk current is observed for the $(PtNPs/CoTMPyP)_9$ multilayer films. The ratio of the ring to disk current, i_R/i_D, is 0.016 for the multilayer films, which is much smaller than the collection of 0.193 determined with the use of the $[Fe(CN)_6]^{3-/4-}$ redox couple under the same solution conditions. From the ratio of the ring−disk current, the calculated number of

(34) Bard, A. J.; Faulkner, L. R. *Electrochemical Methods, Fundamentals and Applications*; Wiley: New York, 1980; p 288 (Chapter 8).
(35) Andrieux, C. P.; Dumas-Bouchiat, J. M.; Savéant, J. M. *J. Electroanal. Chem*. **1982**, *131*, 1.
(36) Kang, C.; Xie, Y.; Anson, F. C. *J. Electroanal. Chem*. **1996**, *413*, 165.
(37) Mano, N.; Fernandez, J. L.; Kim, Y.; Shin, W.; Bard, A. J.; Heller, A. *J. Am. Chem. Soc*. **2003**, *125*, 15290.
(38) Toda, T.; Igarashi, H.; Uchida, H.; Watanabe, M. *J. Electrochem. Soc*. **1999**, *146*, 3750.

electrons involved in the reduction of O_2 is found to be 3.83 according to the equation $n = 4 - 2(i_R/i_D N)$,[39] which is almost identical to that acquired from the Koutecky–Levich plot (vide supra). Taking into account that the rates of H_2O_2 and H_2O production are i_R/N and $i_D - i_R/N$, respectively, the formation efficiency of H_2O can be estimated as follows:[40]

$$P_{(H_2O)} = \frac{N(i_D/i_R) - 1}{N(i_D/i_R) + 1} \quad (6)$$

From the value of i_R/i_D, 0.016, the efficiency of H_2O formation for the $(PtNPs/CoTMPyP)_9$ multilayer films amounts to 85%. This result indicates that the reduction of dioxygen at the $(PtNPs/CoTMPyP)_9$ multilayer film electrode mainly supports the four-electron pathway to produce a low yield of H_2O_2.

3.7. Stability of the Multilayer Films Containing PtNPs. The stability of the as-prepared multilayer films containing PtNPs was determined by comparing the changes in voltammetric peak currents of before and after potential scanning for 2 h between −0.2 and +1.5 V at 50 mV s^{-1} in 0.5 M H_2SO_4. There was no observable decrease in the voltammetric currents of the PtNPs and the catalytic current of dioxygen reduction. Furthermore, no observable change in the shape and height of the current of dioxygen reduction was found, after the as-prepared modified electrode was exposed in air or soaked in the supporting electrolyte for 2 months. The as-prepared multilayer films containing PtNPs are very stable and difficult to remove from the electrode surface. The only way to remove the film is to polish the electrode. The good stability of the multilayer films is very useful in the preparation of the modified electrode and the catalytic reaction. It may make such catalysts very good candidates for use in cathode material of fuel cells.

4. Conclusions

Overall, the present results demonstrate the successful construction of PtNP-containing 3D nanostructured material using metalloporphyrin as a molecule cross-linker by the LBL electrostatic self-assembly technique, which exhibits slightly higher current density and more positive polarization potential for dioxygen reduction than those of the bulk Pt electrode. The preparation method is very simple, controllable, and reproducible. RDE voltammetry and RRDE voltammetry demonstrate that the PtNP-containing films with high stability can catalyze mainly four-electron reduction of O_2 to H_2O in air-saturated 0.5 M H_2SO_4. Furthermore, the responses for dioxygen reduction are dependent on the amount of assembly components in the films, thus, providing an alternative means for tuning their electrocatalytic activity, which can be easily controlled through the variation of the film thickness or more specifically the deposition cycles in the LBL process. This feature makes the multilayer films promising candidates for dioxygen reduction, which has some merits resulting from the advantages of the LBL self-assembly technique, such as simplicity, long-term stability, cheapness, versatility, and so on. These make such catalysts very good candidates for use in diverse conditions and hopefully can replace the metal Pt as the efficient cathode material in fuel cells.

Acknowledgment. This work was supported by the National Natural Science Foundation of China (Nos. 20275036, 2021130506) and by Special Funds for Major State Basic Research of China (No. 2002CB713803).

LA048337S

(39) Liu, S.; Xu, J.; Ran, H.; Li, D. *Inorg. Chim. Acta* **2000**, *306*, 87.
(40) Jakobs, R. C. M.; Janssen, L. J. J.; Barendrecht, E. *Electrochim. Acta* **1985**, *30*, 1085.